UNITED NATIONS UNIVERSITY
UNU-GTP
Geothermal Training Programme

Orkustofnun, Grensasvegur 9,
IS-108 Reykjavik, Iceland

Reports 2017
Number 23

TEMPERATURE AND WELL TEST ANALYSIS OF SELECTED WELLS OF ALUTO LANGANO GEOTHERMAL FIELD, ETHIOPIA

Teka Nigussie Gebru
Ethiopian Electric Power – EEP
Kirkos Kifle Ketema, Wereda 07, House No. 944/05
Meba Building, P.O. Box 15881
Addis Ababa
ETHIOPIA
teka2005@yahoo.com

ABSTRACT

Aluto Langano geothermal area is one of the 22 high-temperature geothermal prospects in the Ethiopian main rift. It has a potential of 70 MWe and has confirmed temperatures greater than 200°C at a depth of 1000 m. Of the 10 deep wells drilled in the area, two are directional, drilled in 2015 to a measured depth of 1921 and 1950 m. The remaining eight wells are all vertical, drilled in the 1980s. The objective of this report is to analyse the temperature and pressure in wells LA-4 and LA-6 in order to estimate the formation temperature of the geothermal system, as well as estimate the reservoir parameters of the field based on well test analysis for wells LA-4 and LA-7. Temperature and pressure data from the warm up period and injection tests are limited. The formation temperatures of the wells were estimated using the Horner method, from which the estimates are usually lower than the actual value. Comparing the latest measurements from 2016 and 2017 and combining with the Horner plot results, gave a more realistic formation temperature. The temperature reaches over 300°C in well LA-6 and 230°C in well LA-4. The main feed zones of well LA-4 are located at 1460 and 1900 m, as indicated by pivot points in pressure logs and confirmed by temperature changes at the same depths. Pivot points in the pressure logs are at 1900 m in LA-6, which indicates a main feed zone confirmed by a slight temperature change at the same depth, but an already defined feed zone at 1600 m from previous studies, was also indicated by temperature change. The injection test was processed in *Welltester* software, which was developed at ISOR to estimate reservoir and well parameters. The data from the injection tests were too scarce to use directly in *Welltester*, so manually adding data where there were gaps, followed by interpolation in *Welltester*, gradually gave good results with respect to the quality of the data. Storativity was of the order of magnitude 10^{-8}, and transmissivity 10^{-8} to 10^{-9}, where the latter one is rather low compared to Icelandic high-temperature geothermal wells. The skin factor was generally negative, which indicates that the permeability in the closest surroundings of the well is higher than farther away. The injectivity index is rather low, between 1.3 and 2.2 (L/s)/bar, which can explain partly, why the wells have not been good producers.

1. INTRODUCTION

Geothermal utilization in Ethiopia began in 1886, when Etege Tayitu, the wife of king Menelik II, built a bathhouse for herself and members of the Showa royal court near the Filwoha hot mineral springs (Wikipedia, 2017). Filwoha is an Amharic term which means "boiled water", and the hot springs are still open to the public. In 1969, geothermal exploration started with regional geo-volcanological mapping and hydrothermal manifestation inventory in most of the Ethiopian Rift that revealed high- and low-enthalpy geothermal resources in the Ethiopian rift valley and Afar depressions (Teklemariam et al., 2000). The Ethiopian government, with technical and financial assistance from the United Nations Development Program (UNDP), then conducted a systematic campaign of geothermal exploration along the main Ethiopian rift and the Afar depression. The Ethiopian rift extends for over 1000 km in a north-northeasterly direction from the Ethiopia-Kenya border to the Red Sea, and covers an area of 150,000 km^2. After several years of exploration activities, which included geological, geochemical and geophysical surveys, 18 geothermal prospecting areas were selected for further feasibility studies through drilling of exploration wells. Recently, a feasibility study was conducted for six out of the 18 geothermal prospects (Figure 1), namely Aluto Langano, Tendaho, Corbetti, Abaya, Tulu Moye, Dofan and Fantale geothermal fields, based on their strategic locations, i.e. proximity to the existing grid and population density (Ministry of Mines and Energy, 2008).

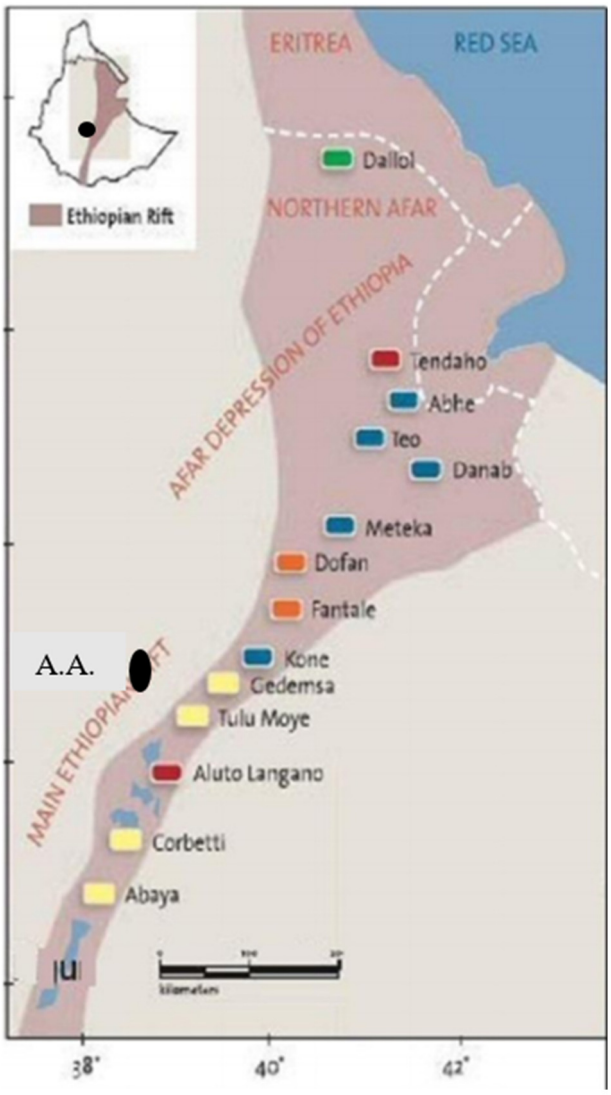

FIGURE 1: Main Ethiopian Rift and geothermal prospect areas of Ethiopia (modified from Hutchison et al., 2015)

Aluto Langano geothermal field has been prioritized due to commercial interest since 1969 by doing several geoscientific investigations resulting in the drilling of eight deep wells in the early 1980s and the commissioning of a small binary power plant with a 7.3 MWe capacity, in operation intermittently from 1998 to 2010. According to ELC (2016), Ethiopian Electric Power and Geological Survey of Ethiopia are in charge of the development of geothermal resources in the country by undertaking a series of geoscientific investigations in Aluto Langano geothermal prospect and other prospects. This exploration work has been financed by different governments and donor organizations, such as the Government of Italy, Government of New Zealand, Government of Iceland (through ICEIDA), Government of Japan (through JICA), United Nations development program (UNDP), World Bank (WB) and Nordic Development Fund (NDF) since 1969. The expected potential of the field is 70 MWe and the geothermal development work is to be split into three phases, Aluto I, Aluto II, Aluto III, which include geological, geochemical and geophysical surveys.

The ambient average air temperature of the Aluto Langano geothermal field is 18°C and the mean annual rainfall may exceed 1000 mm during June to October. The field forms an internal drainage basin of 10 km ×13 km and rises up 500-600 m above the rift floor with a slope of 30% and reaches a maximum elevation of 2328 m a.s.l. in the south western portion (ELC, 2016).

The Aluto Langano geothermal field is believed to cover an area of 100 km^2. A total of 10 deep exploratory wells have been drilled there to a maximum depth of 2500 m. Information about the wells is summarized in Table 1. Eight of the wells (LA-1 to LA-8) are vertical, drilled between 1983 and 1986, but two of them, LA-9D and LA-10D, are the first directional wells drilled in Ethiopia, to a depth of 1920 and 1950 m, respectively, completed in 2016.

Four wells among the earliest wells (LA-3, LA-4, LA-6 and LA-8) of the geothermal field have been used to supply steam and brine to operate a 7.3 MWe binary pilot power plant commissioned in 1999 (Teklemariam et al., 2000). At present, this power plant is non-operational.

The objective of this report is to assess the formation temperature and some reservoir parameters of selected wells from the Aluto Langano geothermal field, using the Horner method and well test analysis software, respectively. Wells LA-4 and LA-6 (Figure 2) are used for formation temperature assessment based on temperature and pressure logs, which were measured during warm up and after discharge of the wells. Wells LA-4 and LA-7 are used for well test analysis where the *Welltester* software is used to manipulate the challenging injection test data collected in the 1980s.

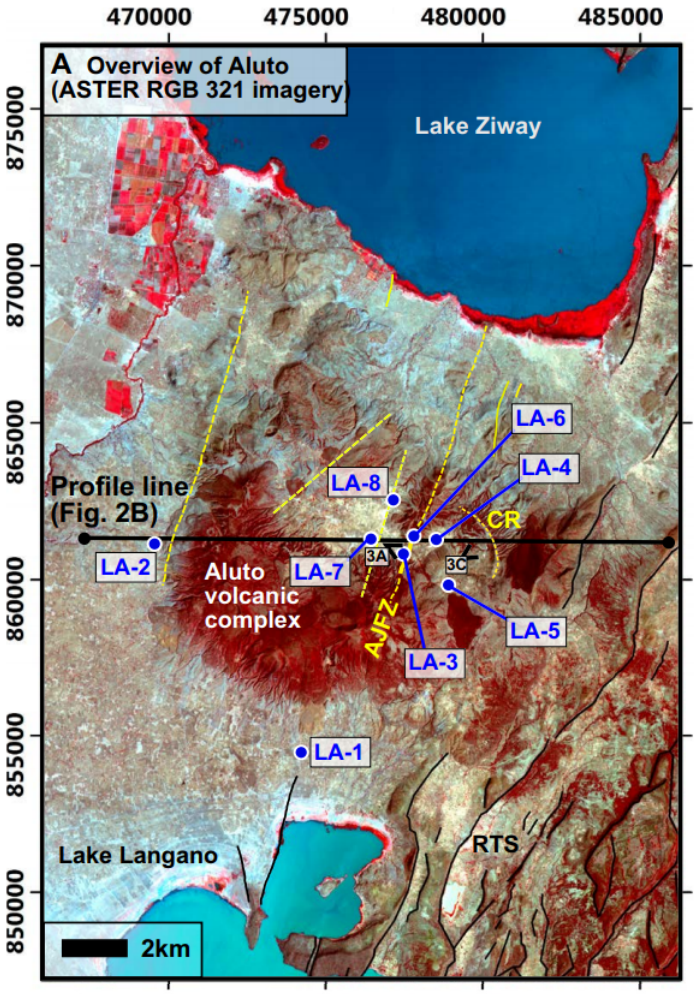

FIGURE 2: Location map Aluto Langano geothermal wells (ELC, 2016)

TABLE 1: Information about exploratory wells located in Aluto Langano geothermal field (ELC, 2016)

Well	WH coordinates		WH elevation	Total mea. depth	Total vert. depth	Elev. of well bottom	Coordinates of well bottom		9⅝ casing shoe	7" slotted liner	Notes
	North	East	m a.s.l.	m	m	m a.s.l.	North	East	MD (m)	MD (m)	
LA-1	853,308	474,047	1601	1317	1317	284	Vertical well		702	800-1317	Sterile w.
LA-2	861,501	469,489	1724	1602	1602	122	Vertical well		892	950-1602	Sterile w.
LA-3	860,723	477,401	1921	2144	2144	-223	Vertical well		748	1035-2140	
LA-4	860,839	478,359	1957	2062	2062	-106	Vertical well		775	746-2035	
LA-5	859,410	478,757	2038	1869	1869	169	Vertical well		752	-	Unpro. w.
LA-6	861,278	477,649	1963	2201	2201	-239	Vertical well		754	1499-2201	
LA-7	860,832	476,296	1891	2449	2449	-558	Vertical well		956	1788-2449	
LA-8	862,190	476,944	1895	2501	2501	-606	Vertical well		721	1867-2464	
LA-9D	860,736	477,863	1956	1920	1784	172	860,849	477,422	605	599-1915	
LA-10D	860,846	477,807	1956	1951	1816	140	861,256	477,409	807	815-1951	

2. GEOLOGICAL SETTING OF ALUTO GEOTHERMAL FIELD

2.1 Geographical location and stratigraphical settings of the study area

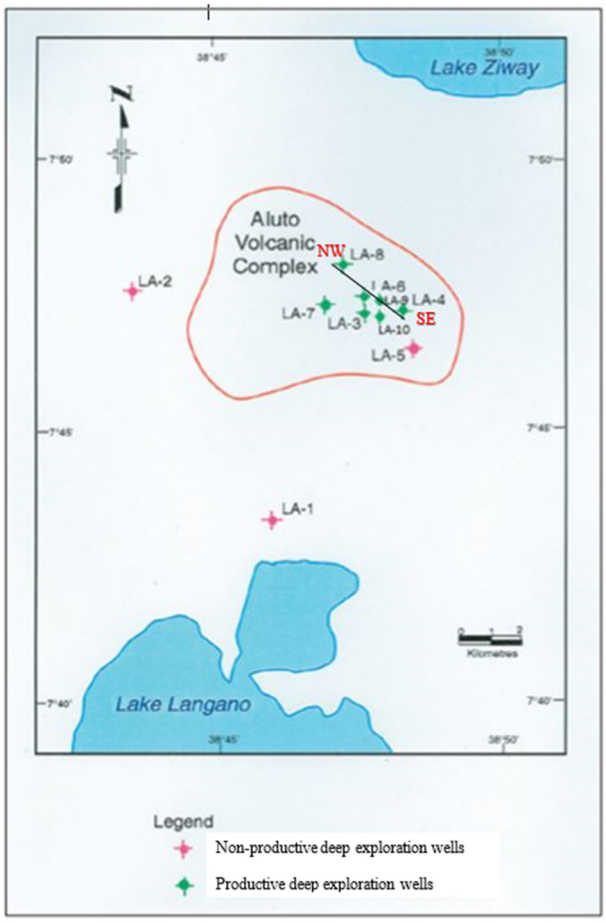

FIGURE 3: Location of Aluto Langano geothermal field (Worku, 2016)

The Aluto Langano geothermal field is located in the Lakes District, Ethiopian main Rift Valley, about 220 km out of Addis Ababa and covers an area of about 100 km^2. It lies between the lakes Langano and Ziway, and rises to about 690 m above the surrounding Adami Tullu Plain. The plain has an elevation of about 1600 m a.s.l. (Figure 3) with a broad truncated base and a summit caldera 6 km × 9 km in area, elongated in a west-northwesterly direction and has formed a basin of internal drainage. Volcanic activity at the Aluto Langano volcanic centre is entirely of Quaternary age and was initiated with a rhyolite dome building phase intervened by explosive pyroclastic pumice eruptions. The young age of these volcanic products indicates a heat source, which is still hot at depth. An extensive cap rock with a large lateral coverage exists at Aluto Langano in the form of lake sediments and it is associated with the overlying pyroclastics. These cap rocks serve to prevent the heat of the Aluto system from escaping to the surface, thus insuring a minimal cooling rate of the geothermal system (Ministry of Mines and Energy, 2008).

The stratigraphical setting of the Aluto Langano geothermal field consists of three main units, with the thickness increasing westwards from 300 to 1000 m. The main units are (ELC, 2016):

1) *Pre-Aluto volcanic products, aged 1.5-3.5 Ma*, which include the Munesa ignimbrite, Bofa basalt, Dima trachyte, Hula Senyo ignimbrite, Kenchere rhyolite and Wenshe Danta basalt, Aluto early volcanic products, and sedimentary formations.
2) *Aluto volcanic products aged 2-150 ka,* which include the Aluto older volcanic units (pre-caldera), Aluto young volcanic unit (syn- and post-caldera) and an obsidian lava flow represents the youngest volcano.
3) *Sedimentary formations* which include Lacustrine deposits which cover a large part of the field varying from sand gravel to fine silt and clay. They are rich in diatomite and colluvial deposits.

2.2 Structural setting of Aluto Langano geothermal field

According to ELC (2016), there are four main directions of tectonic activity, NW-SE, ENE-WSW, NE-SW and NNE-SSW. Fault settings exhibit sub-vertical configurations with a deep angle ranging between 80 and 90°, except for the one with a ENE-WSW trend which has a dip angle up to 45-50°. The NW-SE trend (Red Sea Trend) is of the main geothermal interest since accumulation of magma and formation of central volcanos is recognized to mainly take place in the southwestern sector and to a certain extent along the course of the Bulbula river. The second tectonic direction, ENE-WSW (Gulf of Aden trend) partly controls the configuration of the Aluto caldera elongated in W-E direction. The

NE-SW trend (Ethiopian Rift trend) is predominant and recognized mostly in the southeast outer part of the field, starting from the formation of the main Ethiopian rift up to 1.6 Ma and it affects mostly the older formations. The NNE-SSW trend (Wonji Fault Belt trend) is the fourth main direction of tectonic activity and is associated with the youngest and most active system. It has three important features/ lineaments (Figure 4) namely; Bobessa-Gabiba lineament, which cross-cuts the eastern rim of the caldera; Artu Jawe-Oitu lineament, which cross-cuts the central part of the caldera along which the most productive wells, LA-3 and LA-6, are located; and the Worbota-Adonsha lineament which cross-cuts the western part of the caldera.

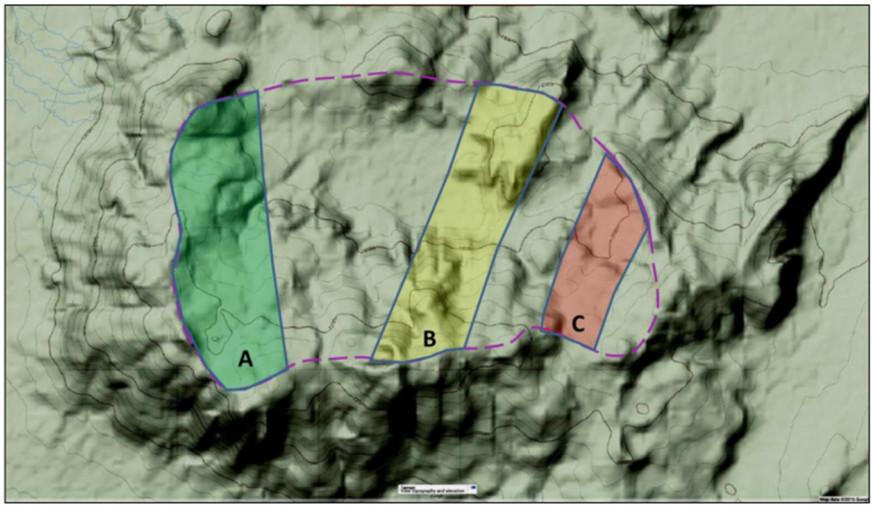

FIGURE 4: Aluto Volcanic Complex (AVC) and the three features of the Wonji Fault Belt trend; A: Worbota-Adonsha lineament; B: Artu-Jawe-Oitu lineament; and C: Bobessa-Gabiba zone (modified from ELC, 2016)

3. TEMPERATURE ASSESSMENT

Stabilized formation temperature is one of the most important parameters to evaluate for a geothermal reservoir, when a well is completed (Hyodo and Takasugi, 1995). Its determination from well logs, requires knowledge of the temperature disturbance produced by circulating drilling mud or fluid (Kutasov and Eppelbaum, 2005). The formation temperature of the wells is estimated using the Horner plot method (Helgason, 1993) which is applied in this report.

3.1 Temperature profiles

Steingrímsson (2013), classified temperature profiles as: linear, inverted, isothermal and boiling point temperature depth profiles. In the linear temperature profile, the heat transfer is dominated by heat conduction and the slope of the temperature log, called the geothermal gradient, is determined by the heat conductivity of the formation and the heat flux through the crust upwards to the surface. Examples of a linear temperature profile measured can be found in the wells in Kaldársel, Vestmannaeyjar and Thorlákshöfn in Iceland (Figure 5). Isothermal formation temperature profiles are found in regions of deep infiltration, circulation, and convection of the fluids, e.g. in the wells in Eyjafjördur, LJ-8, and Reykjavík, RGJ-4 (Figure 5). Boiling formation temperature profiles, the black curved line in Figure 5, are common in geothermal systems with reservoir temperatures in the range of 300°C. These reservoirs are fractured and highly permeable so the heat transfer is dominated by fluid convection and upflow of steam. Inversions in the temperature profiles are sometimes seen in formation temperature curves, such as in well number MG-39 (Figure 5). This is usually explained to be due to horizontal or tilted flow of hot water in the underground. This could be upflow along a non-vertical fracture or that the well is located in the outflow zone of a geothermal reservoir. Temperature reversal is also seen in cold recharge zones of geothermal reservoirs.

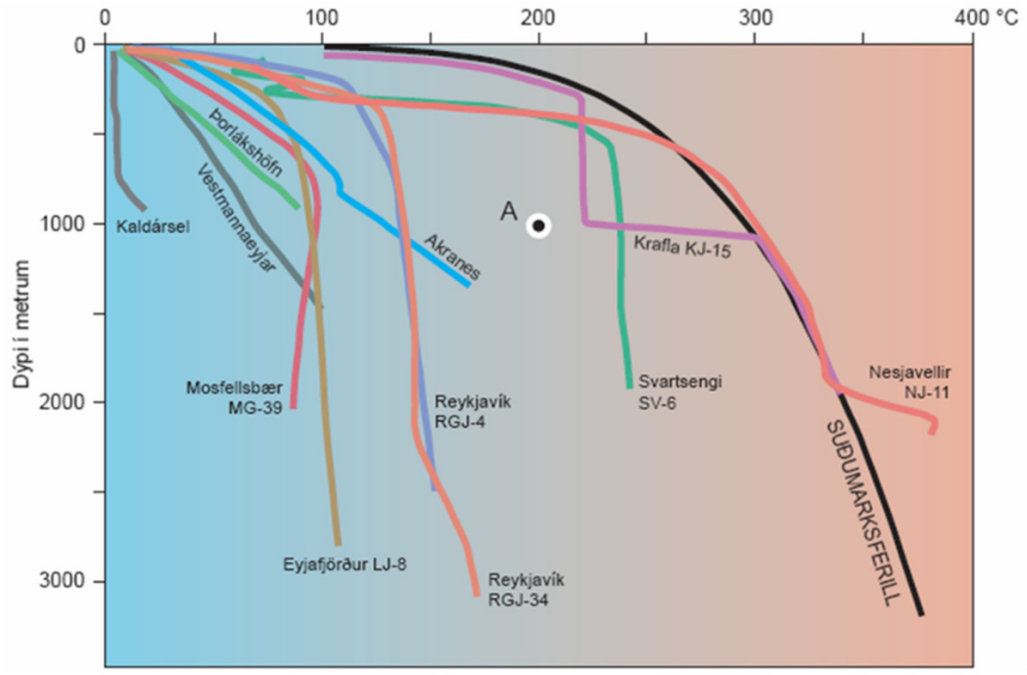

FIGURE 5: Different formation temperature profiles of Icelandic geothermal wells; the thick black curved line represents the boiling formation temperature profile (Steingrímsson, 2013)

3.2 Formation temperature estimation of Aluto Langano geothermal wells

ELC (2016) illustrates briefly the temperature of the Aluto Langano geothermal field. The highest temperature is observed along the axis from LA-3 to LA-6, i.e. along the Jawe lineament, related to the NNE-SSW trending Wonji Fault Belt (Figure 4). This lineament is expected to be responsible for the main upflow in the geothermal system. This is also briefly explained in ELC (1986), as a strong thermal anomaly in the central part of the field along wells LA-3 to LA-8, compared to the regional thermal gradient that is not very high, or less than 100°C/km. The anomaly reaches its peak along the recent north-northeasterly fault system (Wonji fault belt). On both sides of this fault, the anomalous area extends only laterally at intermediate depths (500-1000 m a.s.l.), while at further depth, the wells influenced by lateral flow, LA-4, LA-5, LA-7 and LA-8, show a clear inversion in temperature, and in the case of LA-7 the temperature decreases to almost 100°C. For estimation of the formation temperature, only wells LA-4 and LA-6 are used for the Horner plot analysis.

3.2.1 Horner plot method

The Horner plot method is the most popular method to estimate formation temperature from downhole logging temperature data (Dowdle and Cobb, 1975), whereas Kutasov and Eppelbaum (2005) stated the Horner method to be widely used in petroleum reservoir engineering and in hydrogeological exploration to process the pressure-build-up test data for wells producing at a constant flow rate.

The validity of the Horner plot is based on Fourier's heat conduction equation, which describes the change in temperature (T) as a function of time (t) and position/space (x):

$$c_p \rho \frac{\partial T}{\partial t} = k \frac{\partial^2 T}{\partial x^2} \quad (1)$$

where c_p = Heat capacity of the material (J/m^3°C);
ρ = Density (kg/m^3); and
k = Thermal conductivity (W/m°C).

The Horner plot method is applied below casing depth, where the heat conduction of the formation plays a big role in the temperature of flow based on the heat conduction equation. It uses the measured temperature at a given depth from several temperature logs. The Horner time (τ) is given by Equation 2 below:

$$\tau = \frac{\Delta t}{\Delta t + t_k} \tag{2}$$

where t_k = Circulation time before shut-in (hrs); and
Δt = The time elapsed since the circulation stops (hrs).

The circulation time (t_κ) is an important parameter in the Horner plot method and should therefore be determined accurately. Since drilling (and thus injection of cold fluid) reaches different depths at different times, the circulation time varies with depth, yet the same value is used for all depths. The temperature recovery data is plotted logarithmically with the Horner time and the temperature will gather up as a straight line at infinite time, $\tau = 1$ or $\log \tau = 0$. Figure 6 shows an example of a Horner plot of the evaluation of the formation temperature at 2000 m depth in well LA-6. It is known that the temperature found from a Horner plot is usually lower than the actual formation temperature (H. Tulinius, personal communication, 2017).

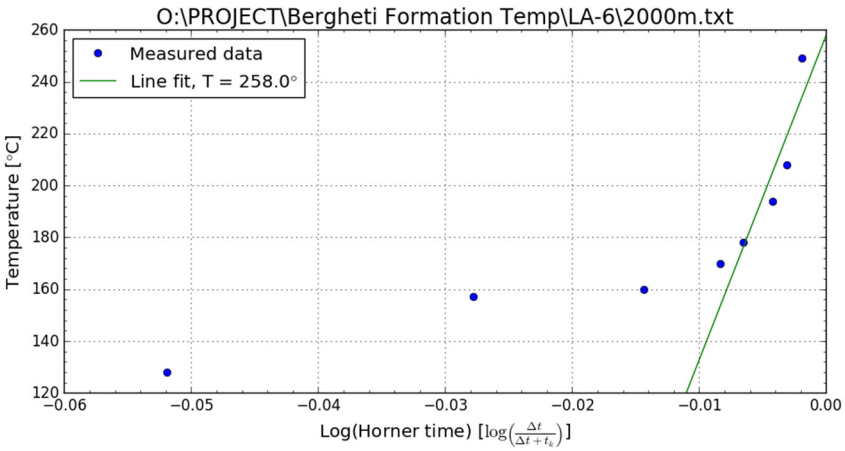

FIGURE 6: Example of a Horner plot to estimate formation temperature of well LA-6 at a depth of 2000 m

3.2.2 Estimation of formation temperature of well LA-4

This well is the fourth deep exploration well drilled in the Aluto Langano geothermal field. It is located at an elevation of 1956 m a.s.l. and the total drilled depth is 2062 m. The drilling started in July 1983 and was completed in October 1983. Major drilling fluid losses occurred at depths of 146-225, 517-558 and 656-674 m. These intervals are all cased off. At 1460-1903 m depth, intermittent partial losses occurred. A gas kick of 7 kg/cm^2 pressure appeared at the head at approximately 610 m depth (Marshet, 1984). The 9⅝" production casing reaches down to a depth of 775 m and the 7" slotted liner starts at a depth of 746 m (Table 1). This also suggests that the fluid in the reservoir remains in liquid phase after the well is opened and the enthalpy of the well is stable at about 950 kJ/kg, which corresponds to saturated water at the permeable layer or aquifer as described in ELC (1986).

The geological formations of the well comprise of Quaternary Aluto pumice, obsidian and pantellerites, Quaternary Aluto trachytic pyroclastics, Pliocene Bofa basalts, Tertiary comenditic pyroclastic and associated silicic lavas. The permeability is apparently associated with the Tertiary ignimbrite at a depth of around 1450 m. The reservoir fluids are saturated with respect to quartz, calcite and fluorite, based on an examination of the alteration mineralogy (Marshet, 1984).

Several temperature logs from a 1-hour warm up period to long periods of warming up were conducted after short injection tests, as shown in Figure 7. As observed from the figure, the measurements are not continuous and the profiles do not show clearly the exact locations of the feed zones. Still, the main feed

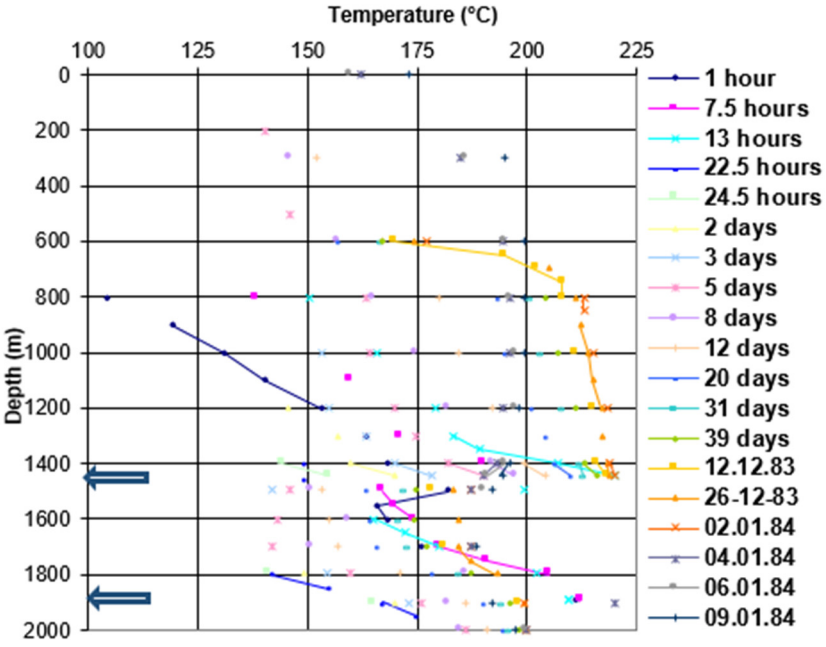

FIGURE 7: Several temperature measurements of LA-4 following an injection test

zones are observed probably at 1450 m, and at 1500-1700 m, as well as many minor feed zones and probably one main aquifer location at around 1900 m depth. UNDP (1987) states that the major permeable/aquifer location appears at a depth of 1445 m, which has a temperature of approximately 230°C, while WestJEC (2016) shows the major permeable zone to appear at around 1650 m with a fluid enthalpy of approximately 959 kJ/kg.

The well is logged in static conditions several times during a warm up period as well as after discharge testing. As observed in Figure 8, the temperature measured during a warm up period is lower than the temperature measured after discharge testing. This could be because the cold drilling water is still stored in the fractured media of the well bore, which affects the temperature measured during the warm up period. The measurements after discharge testing show that the well has not reached equilibrium within 39 days of warm up. As shown in Figure 8, the calculated formation temperature (Horner) of the well is approaching the temperature profile conducted after the discharge test at the depths 800-1400 m and gets lower at the depths below 1400 m. Therefore, the calculated formation temperature in this case shows a minimum temperature, approximately 186-200°C observed at depths of around 1600-2000 m, and a maximum temperature of more than 220°C at depths of around 800-1400 m.

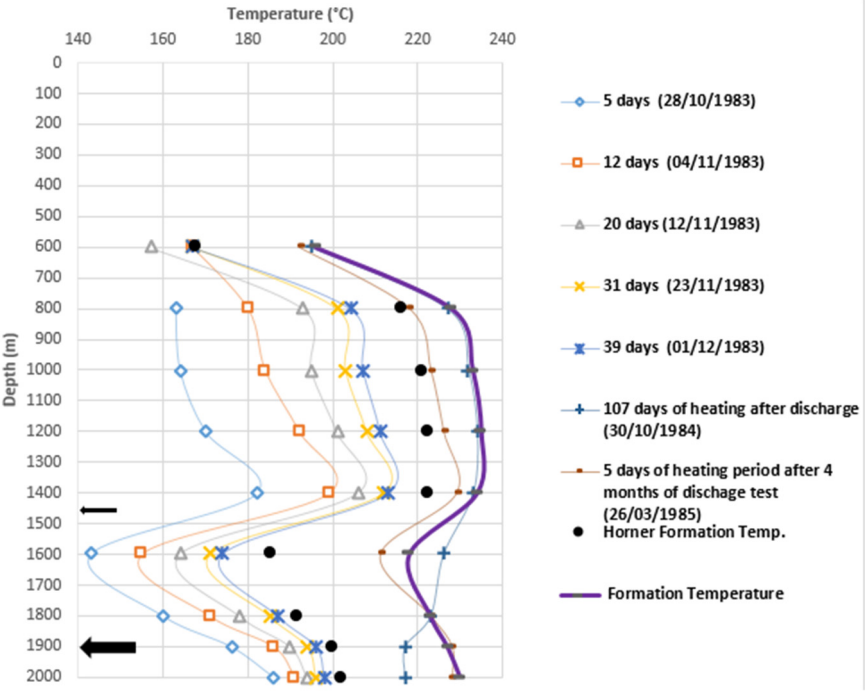

FIGURE 8: LA-4, temperature measurements during recovery period, formation temperature, and temperature profiles after discharge test

The estimated stabilized formation temperature of the well, based on the measurements after discharging, is shown in Figure 8. The temperature is lower than the boiling point curve for a water table at 200 m depth (estimated from the pressure logs in Figure 9), which implies a liquid-dominated reservoir.

It is important to find the pressure pivot point of a well, e.g. the depth of the feed zone that controls the pressure in the well. At this depth, the measured pressure in the well reflects

the actual pressure in the reservoir. In the case of well LA-4, the pivot point is not clearly visible as shown in Figure 9. In order to determine the pivot point, fewer pressure logs are selected as shown in Figure 10. The figure clearly shows two pivot points at the depths of 1460-1500 m and around 1900 m.

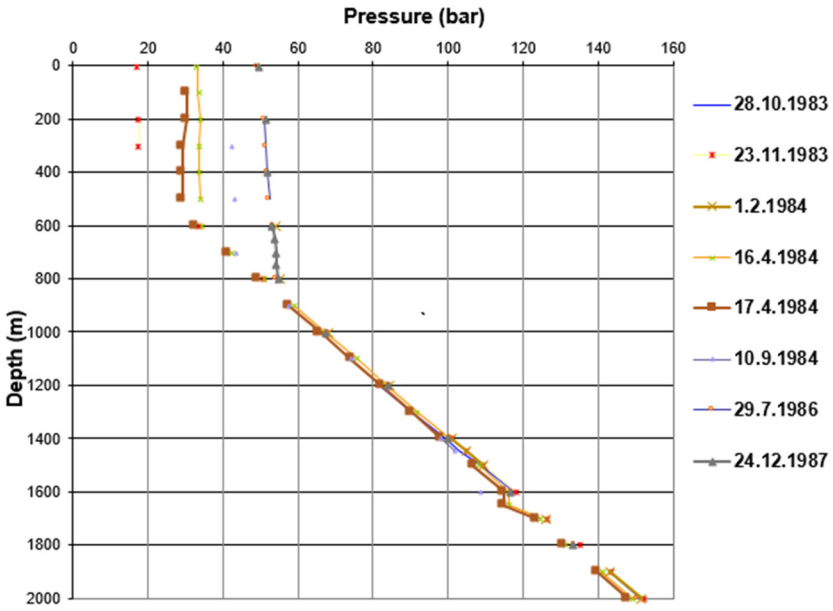

FIGURE 9: Well LA-4, pressure profiles measured in the well

3.2.3 Estimation of formation temperature of well LA-6

According to Ethem Tan (1984), well LA-6 is one of the exploration wells for the Aluto Langano geothermal field, located at an elevation of 1962 m a.s.l. The well was drilled between March and July 1984 to a final depth of 2201 m and complete circulation loss was observed at 2094 m.

Figure 11 shows selected temperature profiles in a static well and to study the formation temperature, selected logs are shown in Figure 12. The temperature is still increasing after a warm up period of 30 days and does not reach stable conditions or equilibrium until after more than one year. This could be because the cold drilling fluid still affects the main feed zones in the well. Probably, cold water flows into the well from the aquifer at 1900 m, which coincides with the pivot point apparent in the pressure logs (Figure 13). After a longer period (> 1 year) of production and shut-in, the temperature of the well reaches equilibrium (Figure 12).

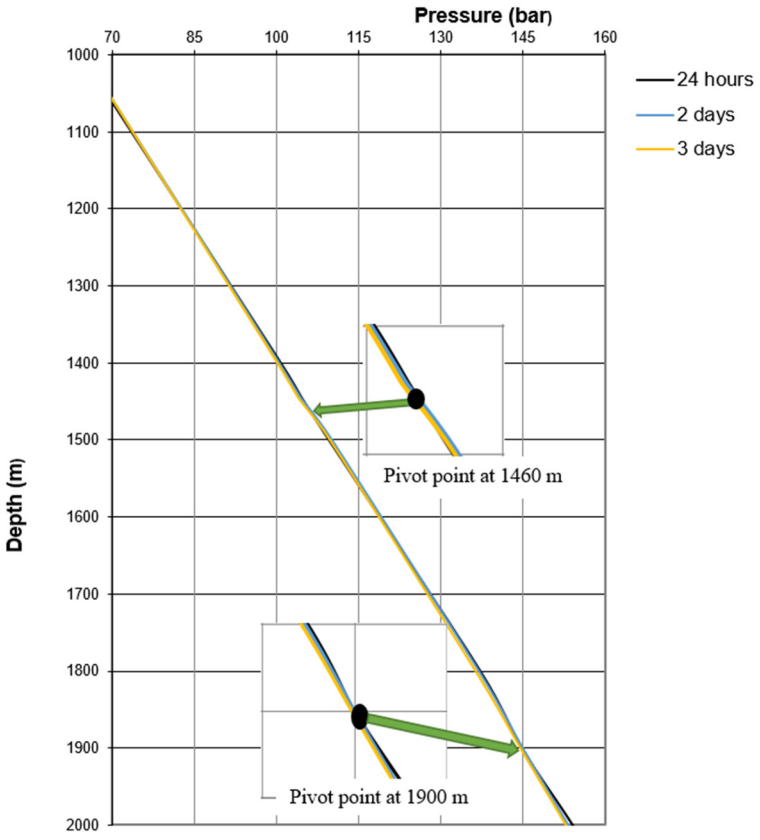

FIGURE 10: Well LA-4, selected pressure profiles showing two pivot points, which are shown separately on the graph

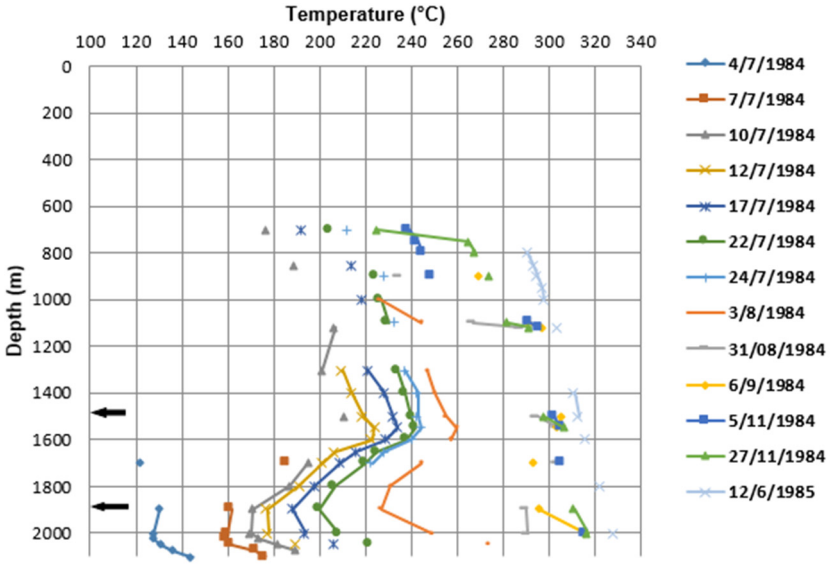

FIGURE 11: Temperature measurements from well LA-6 during warm up; the latest injection test was carried out on 03/07/1984

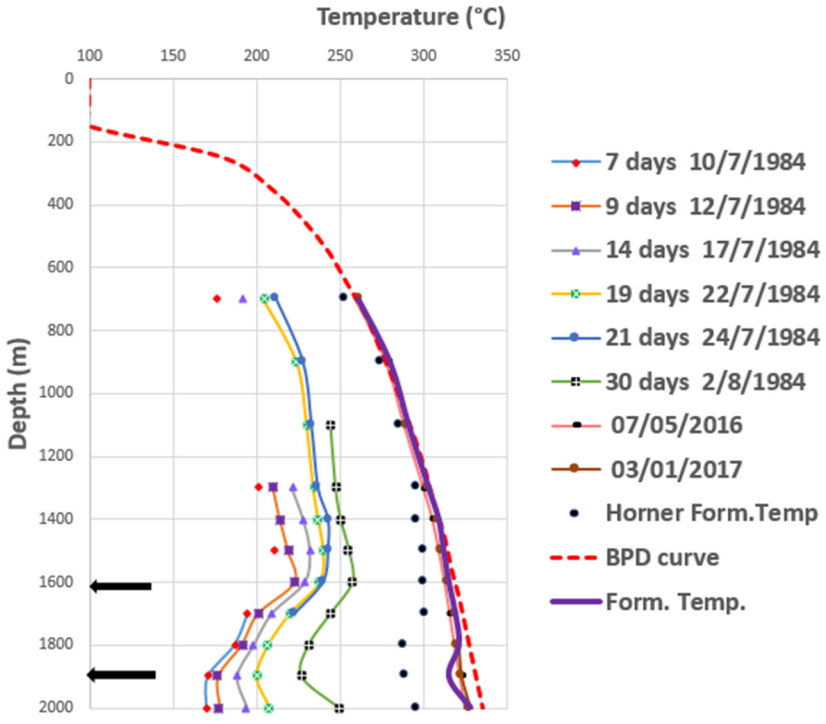

FIGURE 12: Temperature measurements during warm up and estimated formation temperature profiles of well LA-6

Based on the temperature measured during the warm up period, the formation temperature of the well is determined using the Horner plot method, even if the Horner plot gives a minimum estimate for the temperature. Recent temperature measurements from 2016 and 2017 show that the temperature follows the boiling point curve to a depth of approximately 1700 m, where the temperature reaches 300°C. The temperature, calculated with the Horner method, approaches the recent temperature measured at depths between 700 and 1300 m, whereas from 1300 m downward, the Horner estimate is lower than the measured temperature. This implies colder water inflow into the well from aquifers located at depths between 1900 and 2000 m (Figure 12).

The formation temperature shows inversion at a depth of around 1900 m, which indicates cold inflow or inter-zonal flow in the well. The high temperatures observed in the well, following the boiling point curve, support that the well is approaching the upflow zone of the geothermal system.

3.3 Temperature cross-section (SE-NW)

The estimated formation temperatures of wells LA-4, LA-9D, LA-10D, LA-6 and LA-8 are shown in a cross-section from SE to NW (Figures 14, for location see Figure 3). Deducing the formation temperature of wells LA-4 and LA-6 was a part of this project, but the formation temperatures of LA-9D and LA-10D were derived mostly from the latest (January 2017) logging data while LA-8 is based on data from the 1980s. As clearly observed from the cross-section, the hot up flow seems to be in the

vicinity of wells LA-6, LA-9D and LA-10D, which reaches the warmest part (>300°C), probably from the main upflow zone of the reservoir. Well LA-4 is farther away from the warmest part of the reservoir, with temperatures ranging from 210 to 230°C, while well LA-8 is closer to the warmest part of the reservoir. This is probably caused by cold inflow/outflow towards well LA-4 from the eastern escarpment of the rift. The above profile supports the idea, which most authors proposed about the up flow zone location in the vicinity of wells LA-6 and LA-3 (Kebede et al., 2002). The upper clay cap, indicating temperatures less than 140°C is clearly correlating to Figure 14 and extends up to 700-800 m depth, but is cased off in most of the wells.

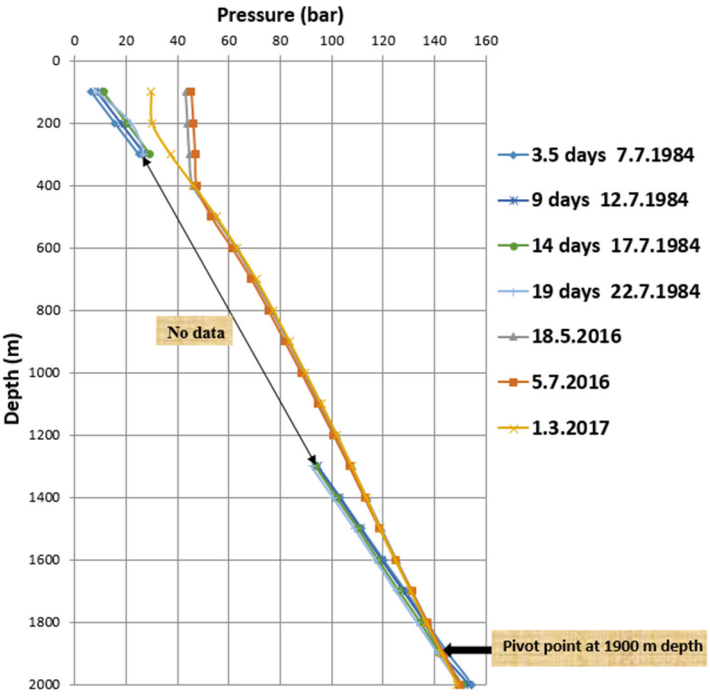

FIGURE 13: Static pressure measurements from well LA-6. A pivot point is observed, which coincides with an aquifer at 1900 m depth. Some profiles are missing data between 300 and 1300 m depth as indicated in figure

4. WELL TEST ANALYSIS

4.1 Introduction

In an injection step test, the injection to a well is increased or decreased in steps while the pressure is monitored at a fixed location and fixed depth. The *Welltester* software (Marteinsson, 2017; Júlíusson et al., 2008; Horne, 1995), which was developed at ISOR for well test analysis, is used to simulate pressure response data, measured during a step test (Figure 15) as a function of time. *Welltester* deduces reservoir parameters and parameters of the well by iterating, starting with guessed parameters and getting closer and closer to the measured pressure.

Axelsson and Steingrímsson, 2012, briefly explain the well test which is a fluid flow test (Figure 15) conducted in geothermal wells to obtain parameters of the reservoir and the well. Well tests are done at the completion of a well, possibly leading to a decision of continuing drilling, but also after a period of production, to see whether and how much the reservoir properties have changed.

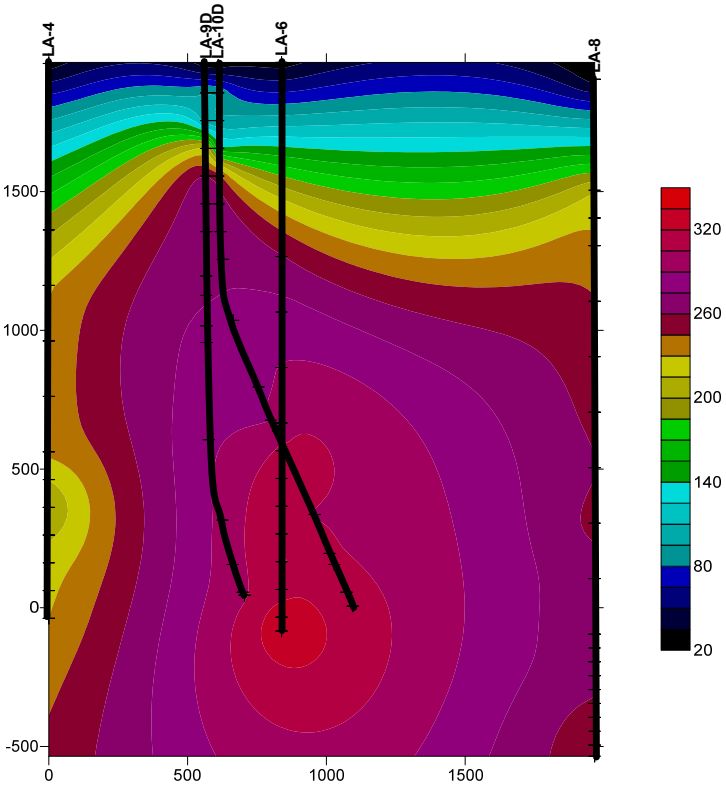

FIGURE 14: Temperature cross-section from southeast to northwest through the system using estimated formation temperature; location of the cross-section is shown in Figure 3

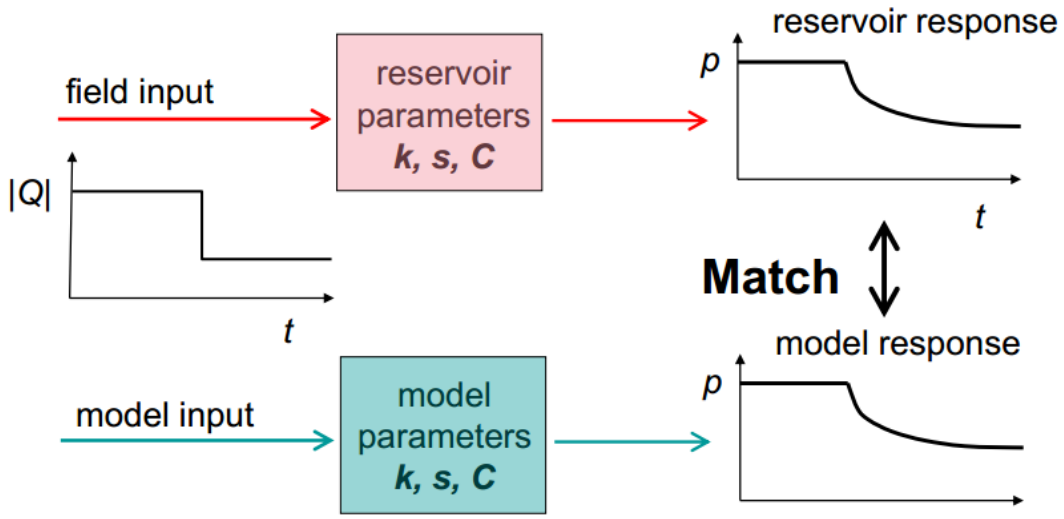

FIGURE 15: Well test analysis procedure (modified by Haraldsdóttir, 2017, from Horne, 1995)

A well test may be analysed using a Theis model (Figure 16) and its variants which assumes a model of homogeneous, isotropic and horizontal permeable layer of constant thickness, confined aquifer, and two-dimensional and horizontal flow towards the producing well, by fitting the pressure response of the model to the measured pressure response data (Axelsson, 2013). In a similar way, the flow in an injection well test is assumed to be horizontal from the well to the surroundings. The possible boundary conditions are illustrated in Figure 17.

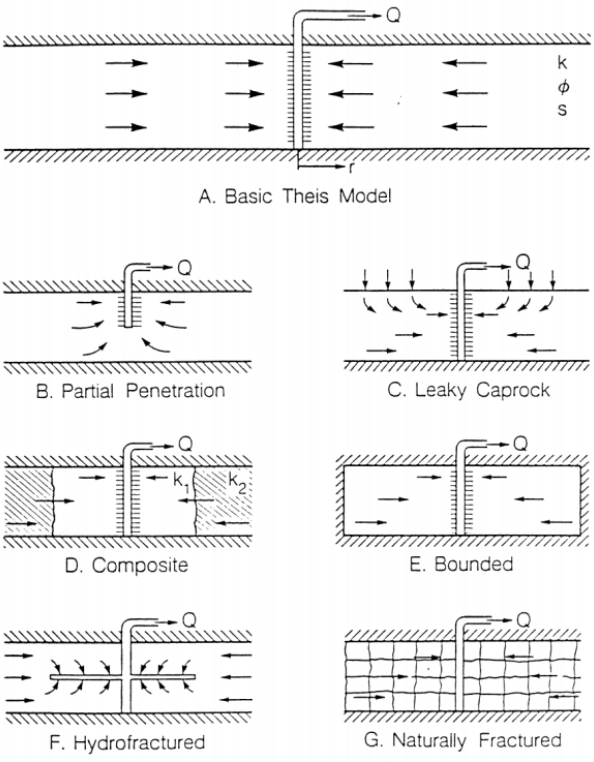

FIGURE 16: A sketch of the basic Theis-model (A) used to analyse pressure transient well-test data along with several variants of the basic model (Bödvarsson and Whiterspoon, 1989)

4.2 Pressure diffusion equation

According to Haraldsdóttir (2017), the pressure diffusion equation is a mathematical description of fluid flow in porous medium and is used to calculate the pressure (p) in the reservoir at a certain distance (r) from the producing well, producing at rate (Q) after a given time (t) (Figure 18). It consists of three main physical principles; the law of conservation of mass, Darcy's law and equation of state of the fluid. There are several assumptions to develop the pressure diffusion equation and these are:

- Horizontal radial flow;
- Darcy's law applies;
- Homogeneous and isotropic reservoir;
- Isothermal conditions;
- Uniform thickness of reservoir (h);
- Single-phase flow;
- Small pressure gradients;
- Small and constant compressibility (c_t);
- Constant porosity (φ);
- Constant fluid viscosity (μ); and
- Constant permeability (κ).

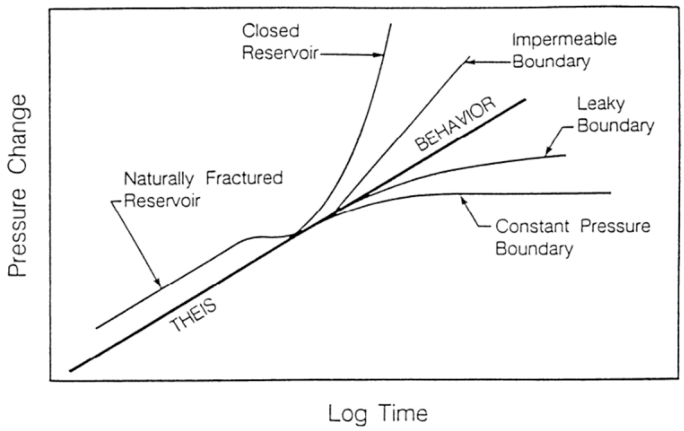

FIGURE 17: Pressure response of a Theis model on a semi-logarithmic plot (linear pressure change vs. logarithmic time) demonstrating the linear behaviour, which is the basis of the semi-logarithmic analysis method (Bödvarsson and Whiterspoon, 1989)

The law of conservation of mass is based on the continuity equation of fluid flow in a porous medium which can be expressed as:

$$Flux\ in - Flux\ out = Increase\ in\ amount\ stored$$

$$\frac{\partial(\rho Q)}{\partial r} = 2\pi r \frac{\partial(\varphi \rho h)}{\partial t} \qquad (3)$$

where Q = Fluid flow, mass introduced (source) or mass removed (sink) (L/s);
ρ = Density of the fluid (kg/m^3);
φ = Porosity of the medium (0-1); and
t = Time (s).

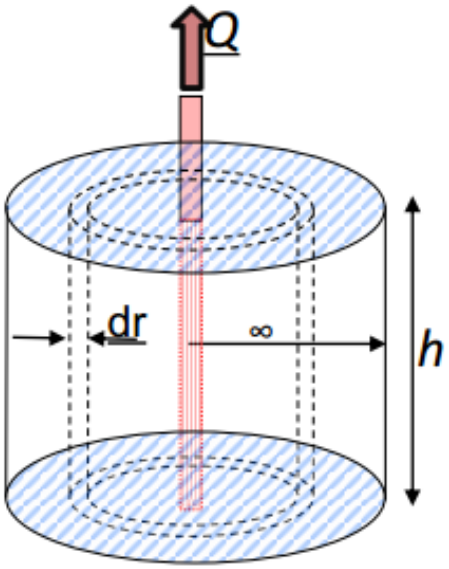

FIGURE 18: Radial flow in a cylinder around a wellbore (Haraldsdóttir, 2017)

The momentum equation (Darcy's law) expresses the fact that the volumetric rate of flow at any point in a uniform porous medium is proportional to the gradient of potential in the direction of flow at that point:

$$Q = \frac{2\pi r k h}{\mu} \frac{\partial p}{\partial r} \qquad (4)$$

where p = Pressure (bar);
r = Radius of investigation (m);
μ = Dynamic viscosity (Ns/m^2); and
h = Reservoir thickness (m).

The third principle is the equation of the state of the fluid (fluid compressibility at constant temperature). The compressibility of a substance is the change in volume per unit volume per unit change in pressure. In a reservoir, which consists of rock (c_r) and pore space occupied by oil, water, and gas (c_w), the total compressibility (c_t) is defined as follows:

$$c_w = \frac{1}{\rho}\frac{\partial(\rho)}{\partial p} \quad ; \quad c_t = \varphi c_w + (1-\varphi)c_r \quad and \quad c_r = \frac{1}{1-\varphi}\frac{\partial \varphi}{\partial p} \qquad (5)$$

Finally, the pressure diffusion equation will be deduced to a one-dimensional second order partial differential Equation 6, which describes isothermal flow of a fluid in porous media, i.e. how the pressure (p) diffuses radially through the reservoir as a function of the distance (r) from the well and the time (t) since the start of production:

$$\frac{1}{r}\frac{\partial}{\partial r}\left(r\frac{\partial p}{\partial r}\right) = \frac{\mu c_t}{k}\frac{\partial p}{\partial t} = \frac{S}{T}\frac{\partial p}{\partial t} \quad or \quad \frac{\partial^2 p}{\partial r^2} + \frac{1}{r}\frac{\partial p}{\partial r} = \frac{\mu c_t}{k}\frac{\partial p}{\partial t} = \frac{S}{T}\frac{\partial p}{\partial t} \qquad (6)$$

Axelsson and Steingrímsson (2012) explain in detail the parameters of the well and the reservoir to be estimated from well-logs during a step-rate well-test and its purpose, which is conducted at the end of drilling a well. Step-tests are done to obtain a first estimate of the possible production capacity of a well

and to estimate its production characteristics. In the case of high-temperature wells, this estimate is only indirect since it is not performed at high-temperature, production conditions. Step-rate well-testing usually lasts from several hours to a few days. Accordingly, Axelsson and Steingrímsson (2012) defines the different well reservoir parameters to be obtained from the testing:

(a) Injectivity index: According to Axelsson and Steingrímsson (2012) define the injectivity index as $II = \Delta Q/\Delta p$, where ΔQ is the change in flow-rate and Δp the change in down-hole pressure, usually based on measured values at the end of each step. In the case of low-temperature wells tested through production step testing, a comparable index is defined, termed productivity index (*PI*). A productivity index is also estimated during production testing of high-temperature wells.

(b) Formation transmissivity or permeability-thickness: Transmissivity can be expressed as $T = kh/\mu$ (or $kh\rho/\nu$), where *k is* the formation permeability, *h* the reservoir thickness, μ and ν the dynamic and kinematic viscosity of the fluid, respectively, and ρ the fluid density. The combining term *kh* is the permeability thickness and its frequently used unit is Dm (Darcy metre).

(c) Permeability (k) is the ability of the reservoir rock to transmit a fluid, which is independent of the fluid properties:

$$k = \frac{K\mu}{\rho g} \tag{7}$$

where K = Hydraulic conductivity (cm/s); and
g = Gravitational acceleration (m/s^2).

The permeability is measured in the unit Darcy (D), or milliDarcy, (mD), where 1 D is equivalent to 0.987×10^{-12} m^2.

According to the report from *Welltester* (Júlíusson et al., 2008), the permeability in geothermal reservoirs is generally on the order of 1-100 mD.

(d) Storativity (S) is explained further in the report on *Welltester* (Júlíusson et al., 2008): "*Storativity varies greatly between reservoir types (i.e. liquid-dominated vs. two-phase or dry-steam) because of its dependence on fluid compressibility* (Grant et.al., 1982). *Common values for liquid-dominated geothermal reservoirs are around 10^{-8} (m^3/Pa m^2) while two-phase reservoirs might have values on the order of 10^{-5} (m^3/Pa m^2)"*:

$$S = c_t h \tag{8}$$

where c_t = Total compressibility (Pa^{-1}); and
h = Reservoir thickness (m).

(e) Skin factor of the well describes an additional pressure drop next to a well due to so-called wellbore damage, often caused by clogging of formation pore-space by drilling mud in the closest vicinity of the well. A negative skin factor, however, reflects a well with stimulated near-well flow, i.e. the permeability is higher than in the surroundings (Figure 19). This could reflect a large surface contact of the well bore with the reservoir, as a result of a fractured, slanted or horizontal well, whereas a positive skin factor shows a damaged zone which has poor contact between the well bore and reservoir because of mud-cake, insufficient perforation density, partial penetration or invaded zone as illustrated in Kushtanova (2015).

Therefore, the skin effect due to damaged or stimulated zone is quantified by the skin factor *s,* which is calculated as (Horne, 1995):

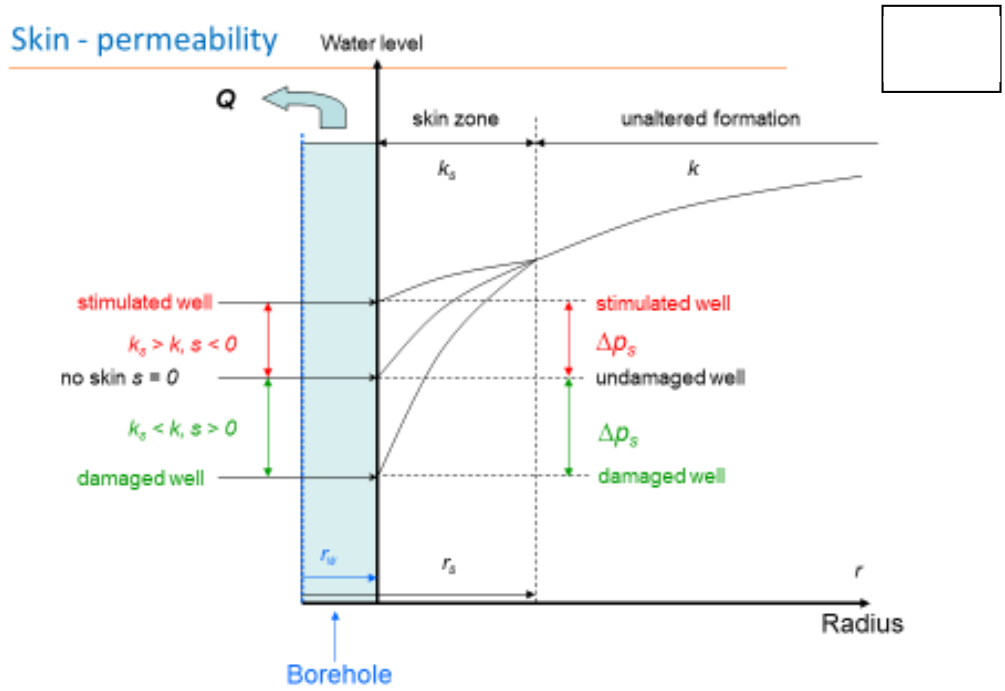

FIGURE 19: The skin effect in the closest vicinity of a well (Haraldsdóttir (2017) modified from Horne (1995))

$$s = \left(\frac{k}{k_s} - 1\right) ln \frac{r_s}{r_w} \tag{9}$$

where k = Reservoir permeability (mD);
k_s = Permeability in damaged or stimulated zone (mD);
r_s = Radius of damaged or stimulated zone, i.e. skin zone (m); and
r_w = Radius of well (m).

(f) *Wellbore storage* (C): This effect can be because of fluid expansion and therefore changing liquid level in the well bore. It depends on wellbore volume and the well-fluid compressibility (Horne; 1995). Therefore, this effect is quantified by:

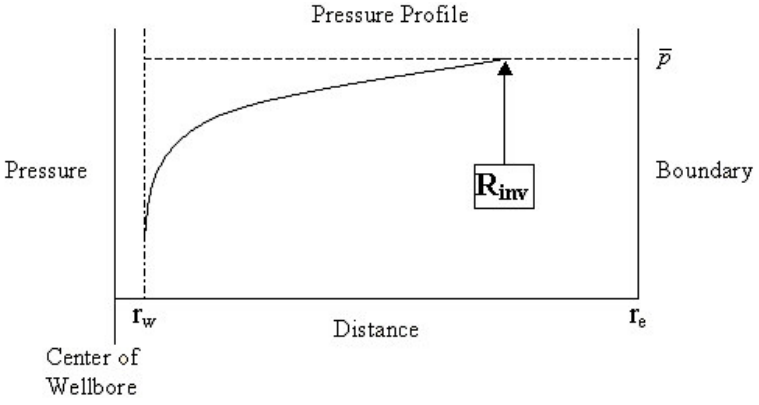

FIGURE 20: A typical well bore radius of investigation (r), r_w is the radius of the well bore, r_e is distance of the boundary of the well, and p is pressure response because of production (Berhe, 2014)

$$C = \frac{V}{\Delta P} \tag{10}$$

where V = The volume of fluid produced from the well bore (m^3); and
ΔP = The pressure drop because of outflow of the fluid from the well bore (Pa).

(g) Radius of investigation (r): The radius of investigation (Figure 20) is the approximate distance at which the pressure response from the well becomes undetectable (Júlíusson et al., 2008).

4.3 Injection step test analysis of well LA-4

After the completion of drilling well LA-4, the injection test was conducted on Oct. 22nd, 1983 by putting the pressure tool at a depth of 1445 m, which was the expected feed point location identified during drilling. The duration of the injection test was approximately 2 hours and 30 minutes with three steps of injection followed by a fall off step lasting 3 hours. Before starting the test there was no injection, i.e. 0 L/s, but in the first step it was 6.6 L/s for 40 minutes, in the second step it was 17.2 L/s for 40 minutes and in the third step the injection rate was 27.5 L/s for 70 minutes, followed by a falloff test for 3 hours. The initial pressure during the first step was 104.5 bar, which increased to 110.1 bar during the second step and then increased to 118.4 bar during the third step. Afterwards it dropped to 105.6 bar during the falloff test. While doing well test analysis, the data as shown in the (Figure 21), is pretty limited and tough to use as input for *Welltester* to simulate. Therefore, preparing the data in two separate files and model them separately in the software is an option for the data correction so that the simulation can be expected to give reasonable results. Here, the pressure response data, particularly for the second and third step, have clearly not been recorded as is shown in Figure 21. Even for the first step and fall off step, the pressure response data are very scarce and it was hard to carry out the well test analysis. As a result, points were added manually in *Welltester* and interpolation was used to fill the gap in the pressure response data (Figure 22).

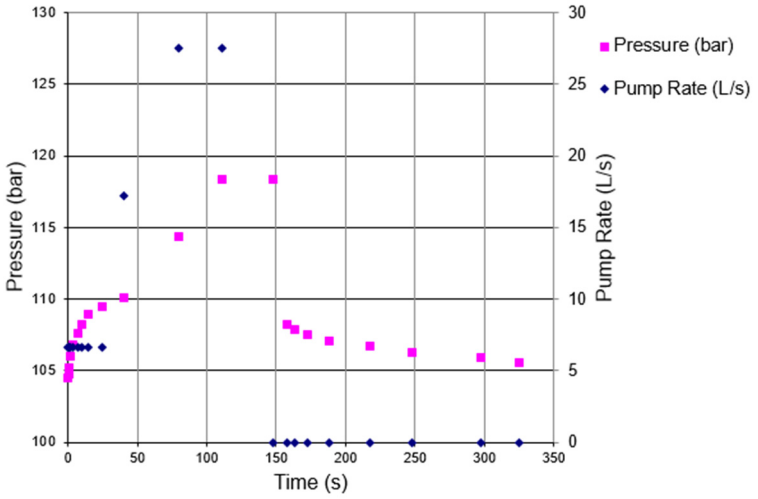

FIGURE 21: Primary data of injection rate and pressure response of LA-4 during injection test

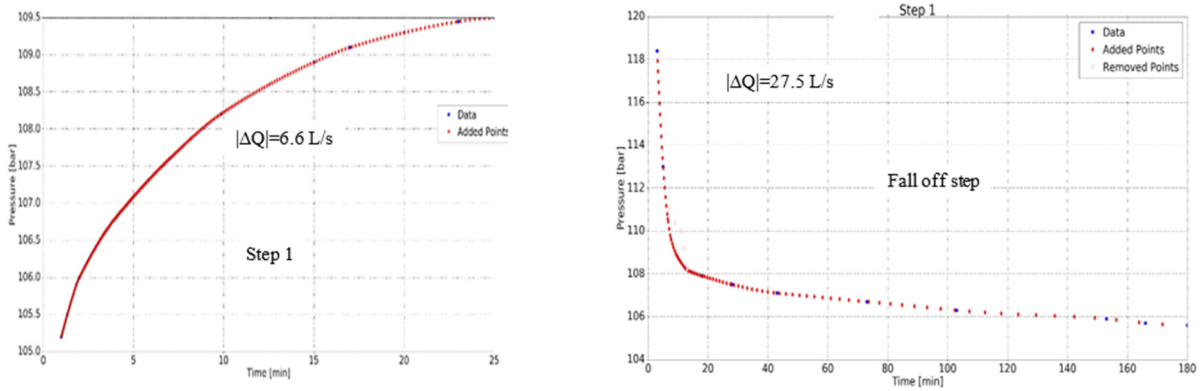

FIGURE 22: LA-4 pressure response (primary data) over time after simple interpolation during injection on a lin-lin graph for a change in injection rate of 6.6 L/s and 27.5 L/s

For the modelling, a temperature value of 215°C was used as described in Woube (1986) but the reservoir pressure is deduced from the data by *Welltester* software (WT). The wellbore radius is inserted, and the user selects the type of formation, basaltic rock, and the porosity after which the software gives the viscosity of the fluid, compressibility of the rock and the fluid and total compressibility (Table 2). The porosity of the reservoir rock here is assumed to be 5% as in ELC (1986) and further explained in ELC (2016).

TABLE 2: Initial reservoir parameters used during well test analysis for LA-4

Reservoir properties	Value	Unit
Reservoir temperature	215	°C
Wellbore radius	0.16	m
Reservoir porosity	5	%
Dynamic viscosity of reservoir fluid	0.000127	Pa s
Compressibility of fissured rock	2.44×10^{-11}	1/Pa
Compressibility of reservoir fluid	9.32×10^{-10}	1/Pa
Total compressibility	6.98×10^{-11}	1/Pa

The model which was selected in *Welltester*, assumes a dual porosity reservoir, constant pressure boundary, constant well bore skin and constant wellbore storage. The response data of the model fits better to the measured data in the fall off step than the data in step 1, as shown in Figure 23 with a log-log scale of pressure and time and Figure 24, which shows the pressure fall off step on log-log scale for pressure and time.

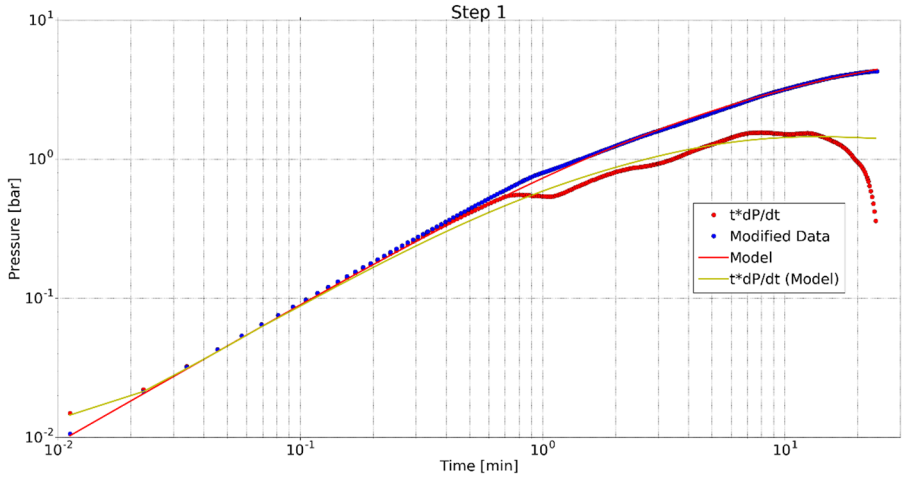

FIGURE 23: LA-4 simulated pressure with time with a model output of a dual porosity reservoir, constant pressure boundary, constant skin and constant wellbore storage for step 1, log-log scale

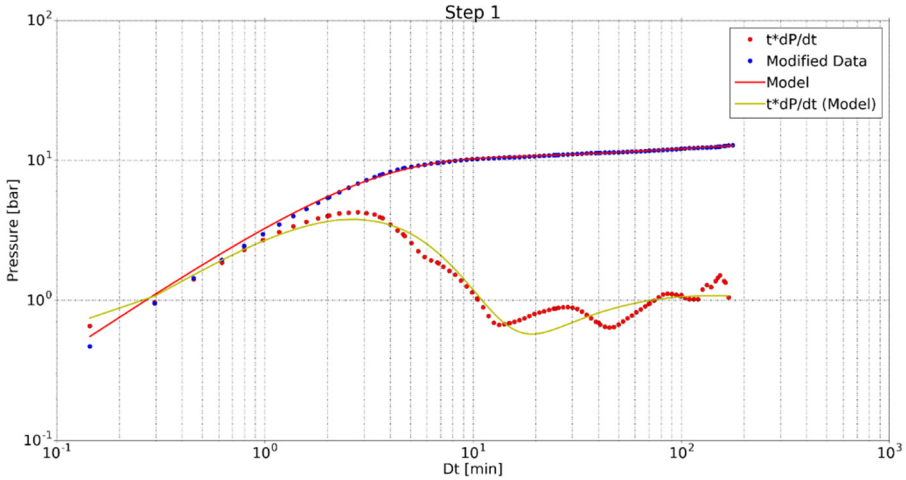

FIGURE 24: LA-4 simulated pressure and model output of a dual porosity reservoir, constant pressure boundary, constant skin and constant wellbore storage for the fall off step, log-log scale

The results from the simulations with *Welltester* are shown in Table 3 for the first step and the fall off step. The coefficient of variation (CV) for the two steps is within reasonable range (low), except for the

storativity (*S*) in the first step and radius of investigation in the fall off step, probably because the data is limited and manually modified and interpolated in the software.

TABLE 3: Well test results from nonlinear regression parameter estimate of dual porosity, constant pressure, constant skin and constant wellbore storage reservoir of well LA-4 for step 1 and the fall off step

Parameter	Step 1		Fall off step		
	Value	CV (%)	Value	CV (%)	Unit
Transmissivity	4.8×10^{-09}	2.8	2.1×10^{-08}	1.1	m³/(Pa s)
Storativity	1.8×10^{-08}	26	3.2×10^{-08}	4.6	m/Pa
Radius of investigation	100	30	250	9	m
Skin factor	-3.0		-0.7		
Wellbore storage	4.3×10^{-06}	2.4	4.2×10^{-06}	- 0.7	m³/Pa
Transmissivity ratio	2.0×10^{-03}	13	2.1×10^{-05}	4.3	
Storativity ratio	1.3×10^{-03}	13	1.1×10^{-03}	5	
Reservoir thickness	260		450		m
Injectivity index	1.5		2.2		(L/s)/bar
Effective permeability	2.4×10^{-15}		5.8×10^{-15}		m^2

4.4 Injection step test analysis of well LA-7

This well is located at an elevation of 1906 m a.s.l. almost 2 km west of well LA-4 and has a maximum drilled depth of 2449 m. The multirate injection test was carried out on Oct. 21st, 1984 by lowering the pressure recording instrument to a depth of 2200 m. The duration of each step was about 1 hour and the test consisted of three steps with pumping rate increased stepwise from 0 L/s to 10.1 L/s in the first step, to 17 L/s in step 2 and 25.9 L/s in step 3 and then reduced to 0 L/s in the fall off step. The total injection test lasted for about 5 hours as a result of stopping of pumping water for about 2 hours because of shortage of water between step 2 and step 3 as is clearly indicated by the gap in the data in Figure 25. The initial pressure of the well in step 1 was 177.1 bar, being increased to 184.4 bar during step 1, then to 194.4 bar during step 2 and finally, after stopping the pumping test for 2 hours and resuming pumping for step 3, the pressure increased to 204 bar. This was used as the initial pressure in the fall off step when it dropped to 184.4 bar. Here, as in the case of LA-4, the primary data is limited (Figure 25) and some manual modification of the data as well as interpolation (Figure 26) in *Welltester* helped prepare the data. Steps 1 and 2 were prepared in one file, step 3 is not used in the analysis and the fall off step was separately prepared in a file as input to *Welltester*.

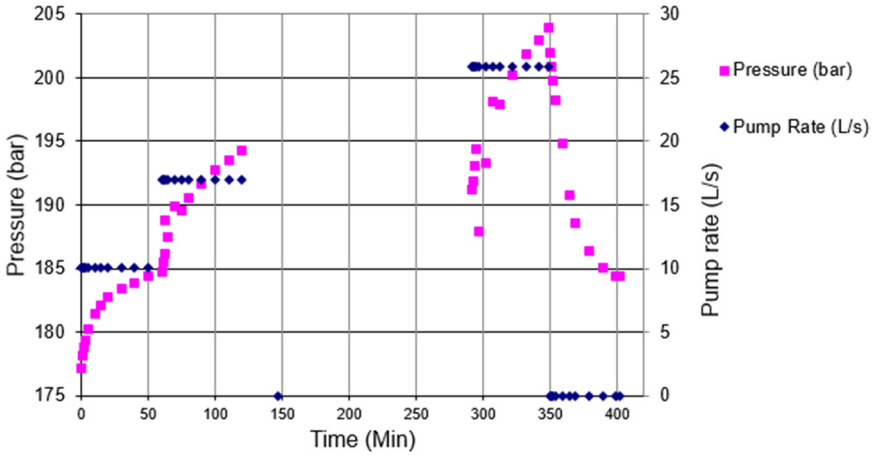

FIGURE 25: Primary data of the injection test of well LA-7, Oct 21st, 1984

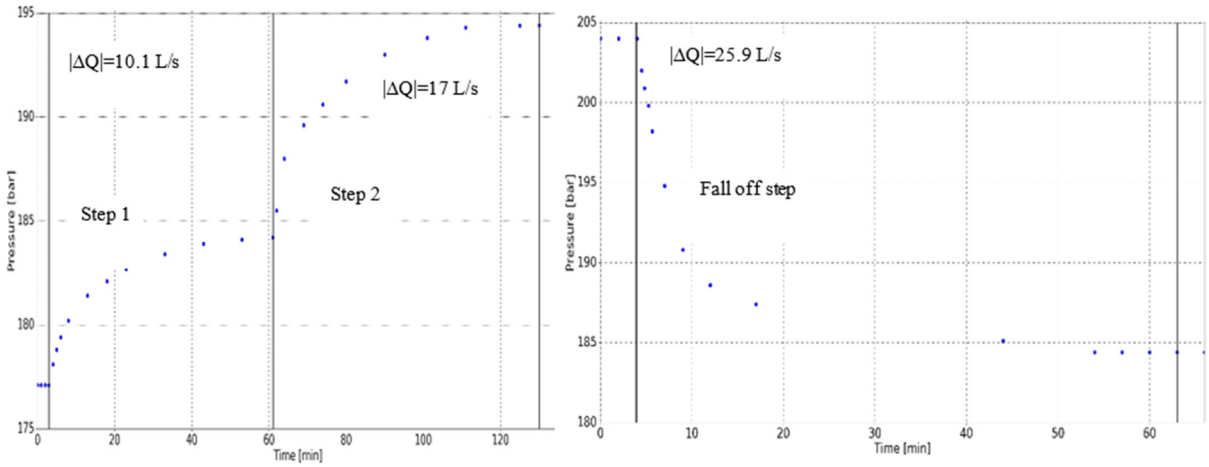

FIGURE 26: Pressure response of LA-7 over time after simple adjustment and interpolation in *Welltester* on a linear graph for steps 1, 2 and the fall off step

The basic assumption for the well test analysis here was the following: a dual porosity reservoir, constant pressure boundary, constant wellbore skin and constant wellbore storage. The initial reservoir parameters, for basaltic rock, used to run the model are shown in Table 4.

TABLE 4: Initial reservoir parameters used in the well test analysis for well LA-7

Reservoir parameters	Value	Unit
Reservoir temperature	220	°C
Wellbore radius	0.16	m
Reservoir porosity	5	%
Dynamic viscosity of reservoir fluid	1.26×10^{-4}	Pa s
Compressibility of fissured rock	2.44×10^{-11}	1/Pa
Compressibility of reservoir fluid	9.28×10^{-10}	1/Pa
Total compressibility	6.96×10^{-11}	1/Pa

The resulting pressure response from the model fits best with the data in the second step as seen in the results in Table 5. Figures 27 and 28 show the results on a log-log scale for step 1 and the fall of step.

TABLE 5: Well test results from a nonlinear regression parameter estimate of a dual porosity, constant pressure, constant skin and constant well bore storage reservoir of well LA-7 for step1, step 2 and fall off step.

Parameter	Step 1		Step 2		Fall off step		
	Value	CV (%)	Value	CV (%)	Value	CV (%)	Unit
Transmissivity	5.6×10^{-09}	1.6	6.0×10^{-09}	1.5	1.6×10^{-09}	36.3	$m^3/(Pa\ s)$
Storativity	9.4×10^{-08}	6.6	1.6×10^{-08}	6.0	0.7×10^{-08}	27.6	m/Pa
Radius of investigation	130	20	200	0.0	210	32.3	m
Skin factor	-2.2		-3.0		-5.5		
Wellbore storage	4.1×10^{-06}	1.5	5.1×10^{-06}	0.73	3.3×10^{-06}	1.2	m^3/Pa
Transmissivity ratio	0.0	5.2	4.8×10^{-04}	5.2	2.0×10^{-05}	11.2	
Storativity ratio	0.03	5.8	3.5×10^{-02}	5.8	4.0×10^{-04}	24.7	
Reservoir thickness	1400		240		100		m
Injectivity index	1.4		1.4		1.3		(L/s)/bar
Effective permeability	5.2×10^{-16}		3.2×10^{-15}		2.0×10^{-15}		m^2

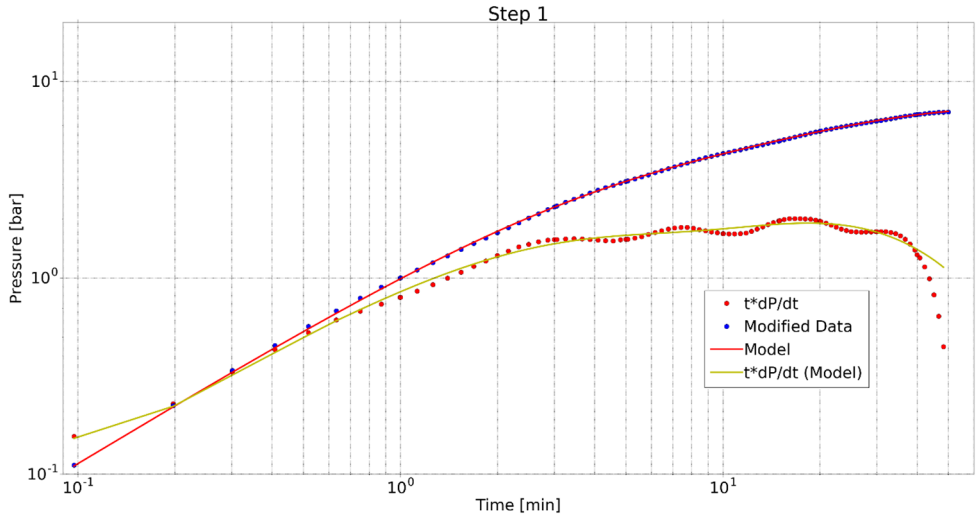

FIGURE 27: LA-7 modified pressure data and model output using dual porosity reservoir, constant pressure boundary, constant skin and constant wellbore storage for step-1, using a log-log scale

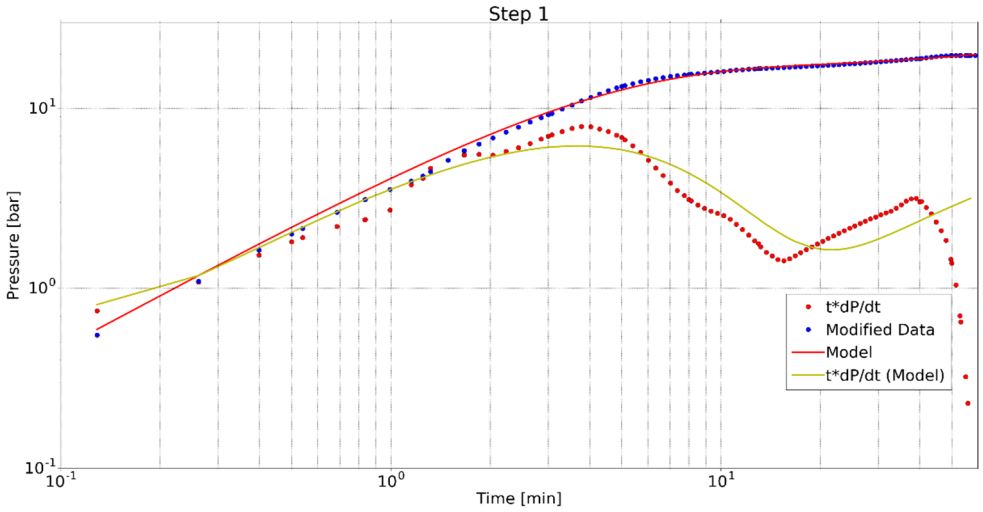

FIGURE 28: LA-7 modified pressure data and model output using dual porosity reservoir, constant pressure boundary, constant skin and constant wellbore storage for the fall off step, using a log-log scale

It is possible to say that based on the coefficient of variation (CV%) in Table 5, the first two steps in the well test analysis have relatively good results, especially with respect to the quality of the data, but the fall off step does not.

The transmissivity value of the well is on the order of 10^{-9} which is smaller than in well tests from Icelandic geothermal wells, that are on the order of 10^{-8} (Júlíusson et al., 2008). The storativity of the well is on the order of 10^{-8} to 10^{-9} which is close to that of Icelandic liquid-dominated reservoirs, which are on the order of 10^{-8} (Júlíusson et al., 2008), but smaller than that of two-phase reservoirs which are on the order of 10^{-5} (Júlíusson et al., 2008). The well test model gives an expected value for the skin factor for an undamaged well, i.e. negative, which is an indication of higher permeability in the skin zone or the closest surroundings of the well, than farther away. Negative skin factor indicates a good connection between the well bore and the reservoir.

The reservoir parameters estimated for well LA-4, using *Welltester* for the well test analysis, show the best fit of the model for the second step. It is slightly better than the best estimate for LA-7, which is the

second step, as the coefficient of variation for the parameters in well LA-4 is smaller than those in LA-7, as shown Table 6.

TABLE 6: Comparison of best estimates of wells LA-4 and LA-7, assuming dual porosity reservoir, constant pressure boundary, constant skin and constant wellbore storage

Parameter	Well LA-4	CV (%)	Well LA-7	CV (%)
	Fall off step		Step-2	
Transmissivity (*T*)	2.1×10^{-08} m^3/(Pa s)	1.1	6.0×10^{-09} m^3/(Pa s)	1.5
Storativity (*S*)	3.2×10^{-08} m/Pa	4.6	1.6×10^{-08} m/Pa	6.0
Skin factor (*s*)	-0.65		-3.0	
Wellbore storage (*C*)	4.2×10^{-06} m^3/Pa	-0.7	5.1×10^{-06} m^3/Pa	0.73
Injectivity index (*II*)	2.2 (L/s)/bar		1.4 (L/s)/bar	
Reservoir thickness (*h*)	450 m		240 m	

5. DISCUSSION

The high temperatures observed in well LA-6 that follow the boiling point curve, show that the well is in the hottest area, as well as wells LA-3, LA-9D and LA-10D which are close by. In terms of temperature, the geothermal field fulfils the criteria to be a good reservoir but the low injectivity indices in the wells as well as the low porosity (WestJEC, 2016) can explain partly why the wells have not been good producers.

The injectivity index (*II*) of well LA-4 in the fall off step (2.2 (L/s)/bar) is not far from the results suggested by ELC (1984), where the injectivity index of the well is estimated to be 25 (L/s)/MPa, which is equivalent to 2.5 (L/s)/bar. However, in the first step the injectivity index is smaller, or 1.5 (L/s)/bar, which may be because of the unavailability of sufficient data. Often, when the injectivity index increases step by step throughout the duration of the injection test, the reason can be clearing in the vicinity of the well.

The pressure response data and its derivative with time indicated a dual porosity reservoir and the simulations in *Welltester* also gave the best results if that model was used for the simulations. ELC (2016) illustrates that the Aluto geothermal field is characterized by a double porosity reservoir and the permeability of the rock matrix is very low. The fluid movement is also controlled by a network of fractures, most likely with limited aperture and density, resulting in a very low permeability.

6. CONCLUSION

Aluto Langano geothermal field is classified as a high-temperature geothermal field as the temperature is greater than 200°C at a depth of 1000 m, which was confirmed in this project. The main conclusions can be summarised as follows:

- The formation temperature reaches over 300°C in LA-6 and 230°C in LA-4. The latter one was drilled in the eastern and colder part of the geothermal field but wells LA-6, LA-9D and LA-10D were drilled in the warmest part of the field. This confirms results already shown in previous reports about the Aluto Langano geothermal field (ELC, 2016, WestJEC, 2016).
- Two possible pivot points were found in selected pressure logs in LA-4, at 1460 and 1900 m depth and the temperature logs show slope changes at the same depths. This confirms the previous results of main feed zones at these depths.

- A pivot point was found in selected pressure logs in LA-6 at 1900 m depth and the temperature logs show a slope change at the same depth. This confirms the previous results where one of the main feed zones was found from temperature logs at this depth. Another feed zone had been deduced at 1600 m depth which was confirmed in the temperature logs in this study.
- The *Welltester* software used in this project to manipulate and analyse the injection step tests was helpful in estimating the reservoir parameters of the wells. The results from the analysis in wells LA-4 and LA-7 were fairly good, especially with respect to the limited data. After manually fixing the data and using interpolation, the best simulations were for a dual porosity reservoir, constant pressure boundary and constant skin.
- The transmissivity and storativity of wells LA-4 and LA-7 were found to be on the order of 10^{-8}-10^{-9}, which is similar or lower than in Icelandic geothermal wells, where they are on the order of 10^{-8}.
- Aluto Langano is classified as a high-temperature geothermal field but the injectivity index is rather low, in the range of 1.0-2.4 (L/s)/bar, which indicates that the wells are perhaps not very well connected to the reservoir. Low values of transmissivity indicate low permeability of the system. The field is therefore not necessarily a good producer in spite of the high temperature. This is in agreement with results of WestJEC (2016).

7. RECOMMENDATIONS

Based on the results and conclusions of my work, I recommend the following activities to be included in the future drilling.

1. Successful future production wells should be drilled to a depth of more than 2000 m. A good location is expected to be along the Wonji Fault Belt, where e.g. well LA-6 is located and the maximum temperature in that area has been observed. Exploration wells clearly give the best information available about a field, and together with results from previous surface exploration, including knowledge about fractures and indication of further warm areas, should be an aid in locating future wells.
2. The data used for the well test analysis in this report were limited, so some recommendations should be made for doing injection tests in wells. First, sufficient amount of water should be stored in a reservoir pond and the pressure measuring instrument should be placed close to the expected main feed zone or between feed zones in case there are two main feed zones. The duration of a multi-step injection test should preferably be 3 hours for each step or at least one of them, in order to get enough pressure response data to be able to identify the effect of the boundary. The duration of steps could be reconsidered, depending on the experience for each field.
3. To estimate the natural state formation temperature of the well, it would be best to do temperature and pressure logging frequently during the first part of the warm up period, followed by logging every other month, preferably for up to a year.

ACKNOWLEDGEMENTS

I want to express my deepest gratitude to the United Nations University Geothermal Training Programme (UNU-GTP), the Government of Iceland and Ethiopian Electric Power (EEP) for allowing me to attend this training. I want to thank Mr. Lúdvík S. Georgsson, Director of UNU-GTP and Mr. Ingimar G. Haraldsson, Deputy Director, Ms. Thórhildur Ísberg, School Manager, Mr. Markús A.G. Wilde, Service Manager and Ms. Málfríður Ómarsdóttir, Environmental Scientist for their dedication towards making us well educated.

My special thanks go to my supervisors, Dr. Svanbjörg H. Haraldsdóttir and Ms. Saeunn Halldórsdóttir, for their careful guidance and supervision and for their patience and support during the time this project was carried out. I would like to thank Mr. Benedikt Steingrímsson for his valuable comments. I would also like to thank Mr. Kjartan Marteinsson for his support and guidance in the use of software developed at ÍSOR, and to all the staff of ÍSOR for the teaching.

I want to say thanks to the geothermal project manager of EEP, Mr. Fikru W/Mariam, for his recommendation to attend this fellowship program.

I would like to thank my parents and family, especially my wife Senait Gesesse and my son Neamin Teka. You endured my long absence. It would have been impossible for me to go through this training without your support, prayers and encouragement.

Last, but not least, I want to thank all the 6-month, MSc and PhD Fellows of UNU-GTP for the memorable time we spent during the stay.

REFERENCES

Axelsson, G., 2013: Geothermal well testing. *Presented at "Short Course V on Conceptual Modelling of Geothermal Systems", organized by UNU-GTP and LaGeo, in Santa Tecla, El Salvador*, UNU-GTP SC-16, 30 pp.

Axelsson, G. and Steingrímsson, B., 2012: Logging, testing and monitoring geothermal wells. *Proceedings of "Short Course IV on Geothermal Development and Geothermal Wells", organized by UNU-GTP and LaGeo, in Santa Tecla, El Salvador,* UNU-GTP SC-14, 20 pp.

Berhe, G.O., 2014: *Correct sampling of gas condensate reservoir with liquid drop around the well.* Stavanger University, Faculty of Science and Technology, Stavanger, MSc thesis, 79 pp.

Bödvarsson, G.S., and Witherspoon, P., 1989: Geothermal reservoir engineering. Part I. *Geothermal Science and Technology, 2,* 1-68.

Dowdle, W.L., and Cobb, W.M., 1975: Static formation temperature from well logs – an empirical method. *J. Petroleum Technology, 27,* 1326-1330.

ELC, 1984: *Installation of back pressure unit, evaluation on Ethiopian Lakes District geothermal fields.* Electro Consult – ELC, Milan, Italy, unpublished report.

ELC, 1986: *Exploitation of Aluto-Langano geothermal resources, feasibility report.* Electro Consult – ELC, Milan, Italy, unpublished report, 283 pp.

ELC, 2016: *Geothermal surface exploration in Aluto-Langano, Ethiopia. Conceptual model report.* Electro Consult – ELC, Milan, Italy, report, 141 pp.

Ethem Tan, 1983: *Final drilling report of LA-4, Langano geothermal field, Lakes District of Ethiopia.* Ministry of Mines, Ethiopia, 21 pp.

Ethem Tan, 1984: *Final drilling report of LA-6, Langano geothermal field, Lakes District of Ethiopia.* Ministry of Mines, Ethiopia, 19 pp.

Grant, M.A., Donaldson, I.G., and Bixley, P.F., 1982: *Geothermal reservoir engineering*. Academic Press, New York, 369 pp.

Haraldsdóttir, S.H., 2017: *Well testing theory – injection.* UNU-GTP, Iceland, unpublished lecture notes.

Helgason, P., 1993: Step by step guide to BERGHITI. User's guide. In: Arason, Th., Björnsson, G., Axelsson, G., Bjarnason, J.Ö., and Helgason, P., 2004: *ICEBOX – geothermal reservoir engineering software for Windows, a user's manual*. ÍSOR – Iceland GeoSurvey, Reykjavík, report ISOR-2004/014, 80 pp.

Horne, R. N. 1995: *Modern well test analysis: a computer aided approach* (2nd ed.). Petroway Inc., Palo Alto, Ca, 257 pp.

Hutchison, W., Tamsin, A., Mather, D.M., Pyle, J.B., and Yirgu, G., 2015: Structural controls on fluid pathways in an active rift system: a case study of the Aluto volcanic complex. *Geosphere, 11-3*, 542–562.

Hyodo, M., and Takasugi S., 1995: Evaluation of the curve-fitting method and the Horner plot method for the estimation of the true formation temperature using temperature recovery logging data. *Proceedings of the 20th Workshop on Geothermal Reservoir Engineering, Stanford University, Stanford, Ca,* 7 pp.

Júlíusson, E., Grétarsson, G.J., and Jónsson, P., 2008: *WellTester 1.0b, user's guide*. ÍSOR – Iceland GeoSurvey, Reykjavík, 27 pp.

Kebede, Y., Kebede, S., Teklemariam, M., and Amdeberhan, Y., 2002: *Compiled summary report on Aluto Langano geothermal field.* Geological Survey of Ethiopia, Addis Ababa, unpubl. report, 141 pp.

Kushtanova, G.G., 2015: *Well test analysis.* Kazan Federal University, Institute of Physics, Department of Radioelektronics, Kazan (Volga Region), Russia, unpublished lecture notes.

Kutasov, I.M., and Eppelbaum, L.V., 2005: Determination of formation temperature from bottom-hole temperature logs. *J. Geophysics and Engineering, 3-4*, 8 pp.

Marshet, Y., 1984: *The petrogenesis, chemistry and hydrothermal mineralogy of rocks in the Langano-Aluto geothermal system, Ethiopia*. University of Auckland, Geothermal Institute, NZ.

Marteinson, K., 2017: *Well Tester user manual, version 2.* ÍSOR - Iceland GeoSurvey, Reykjavík, short report, ÍSOR-17050, Reykjavik, 12 pp.

Ministry of Mines and Energy, 2008: *Investment opportunities in geothermal energy development in six selected geothermal prospects in Ethiopia.* Ministry of Energy and Mines, Addis-Ababa, Ethiopia.

Steingrímsson, B., 2013: Geothermal well logging: temperature and pressure logs. *Proceedings of "Short Course V on Conceptual Modelling of Geothermal Systems", organized by UNU-GTP and LaGeo, in Santa Tecla, El Salvador*, UNU-GTP SC-16, 16 pp.

Teklemariam, M., Beyene, K., Amdeberhan, Y., and Gebregziabher, Z., 2000: Geothermal development in Ethiopia. *Proceedings of the World Geothermal Congress 2000, Kyushu-Tohuku, Japan,* 6 pp.

UNDP, 1987: *Report on project findings and recommendations of Aluto geothermal field, Ethiopia.* UN Department of Technical Cooperation and Development, 97 pp.

WestJEC, 2016: Resource assessment report on Aluto Langano geothermal field. WestJEC, appraisal project, Ethiopia, unpubl. report, 258 pp

Wikipedia 2017: *History of geothermal in Addis Ababa, Ethiopia.* Wikipedia, website: *en.wikipedia.org/wiki/Addis_Ababa.*

Worku S., S., 2016: *Sub-surface geology, hydrothermal alteration and 3D modelling of wells LA-9D and LA-10D in the Aluto Langano geothermal field, Ethiopia*. University of Iceland, MSc thesis, UNU-GTP, report 6, 95 pp.

Woube, Z., 1986: *Analysis of well test data from Langano-Aluto geothermal field, Ethiopia.* UNU-GTP, Iceland, report 11, 50 pp.